

Identification of trace metal pollution in urban dust from kindergartens using magnetic, geochemical and lead isotopic analyses



Zongmin Zhu ^{a,*}, Guangyi Sun ^{a,b,c}, Xiangyang Bi ^a, Zhonggen Li ^d, Genhua Yu ^a

^a State Key Laboratory of Biogeology and Environmental Geology, China University of Geosciences, Wuhan 430074, China

^b Hei Longjiang Institute of Geological Survey, Harbin 150036, China

^c Faculty of Earth Sciences, Northeast Petroleum University, Daqing 163318, China

^d State Key Laboratory of Environmental Geochemistry, Institute of Geochemistry, Chinese Academy of Sciences, Guiyang 550002, China

HIGHLIGHTS

- Magnetic measurements were combined with geochemical and Pb isotopic analyses.
- Magnetic properties showed more prominent values of I_{geo} than those of individual metals.
- Metal pollution sources were identified by Pb isotopes and PCA.
- Industrial emissions and coal combustion are major metal pollution sources in urban areas.

ARTICLE INFO

Article history:

Received 27 November 2012

Received in revised form

15 April 2013

Accepted 16 April 2013

Keywords:

Environmental magnetism

Trace metals

Stable Pb isotopes

Urban dust

Source identification

ABSTRACT

In the present study, magnetic measurements were combined with geochemical analysis and stable Pb isotopic ratios to reveal the distribution and origination of trace metal pollutants in kindergarten dusts from a typical urban environment of Wuhan, central China. The geoaccumulation index (I_{geo}) of magnetic properties was more prominent than those of individual metals. The magnetic susceptibility (MS) and trace metals (Zn, Pb, and Cu) in this study together with published results from other Chinese cities formed a liner relationship, suggesting that metal contaminants in Chinese urban areas had similar MS to metal ratios, which could be used as an indicator for identification of pollution sources between Chinese cities and the other Asian cities. Stable Pb isotopic ratios (1.1125–1.1734 for $^{206}\text{Pb}/^{207}\text{Pb}$ and 2.4457–2.4679 for $^{208}\text{Pb}/^{207}\text{Pb}$) in the urban dusts from Wuhan were characterized by higher ^{208}Pb component in comparison with those from other Chinese cities. This result combined with principal component analysis (PCA) indicated that metal pollutants in the dusts were derived from industrial activities and coal combustion, whereas the traffic emissions were no longer a predominant pollution source in urban environment. Our study demonstrated that environmental magnetic methods could not only reveal the overall situation of trace metal contamination, but also prove evidence in the identification of pollution sources.

© 2013 Elsevier Ltd. All rights reserved.

1. Introduction

Trace metal pollutants have received increasing attention in recent decades due to their potential adverse health effects to humans and widespread existence in urban environment as a result of rapid urban expansion. Atmospheric deposited dust in urban settings is an important carrier of trace metal contaminants. The intensified human activities such as industrial operations, traffic, fossil fuel combustion, and municipal waste disposal, have

produced large quantities of metal particles, which could eventually settle down in urban dust. Through resuspension-inhalation, hand-mouth ingestion and dermal contact, trace metals contained in urban dust could enter human bodies and endanger human's health, especially children's (Roels et al., 1980; Ferreira-Baptista and De Miguel, 2005; Zheng et al., 2010; Soto-Jiménez and Flegal, 2011). For example, many studies indicated that there is a significant correlation between the blood lead levels (BLLs) of children and Pb concentration in urban dust/soil (Laidlaw et al., 2005; Laidlaw and Taylor, 2011). A recent research from the Pearl River Delta region, China, demonstrated that lead contaminated residential dust could be the primary driving mechanism of child blood lead exposure in this area (Chen et al., 2012). Considering the

* Corresponding author. Tel.: +86 27 67883001; fax: +86 27 67883002.

E-mail address: zhumin@cug.edu.cn (Z. Zhu).

high threat of dust metals to children, dusts deposited in kindergartens should deserve more attention since they can be easily contacted by children during their daily outdoor activities.

The contaminated extent and toxicity of trace metals are generally assessed by their total concentrations and speciation, which are usually determined by chemical analysis (e.g., AAS, ICP-AES, and ICP-MS). In addition to the direct but time-consuming chemical approaches, environmental magnetic methods (e.g., magnetic susceptibility and saturation isothermal remanence – SIRM) have also been used to rapidly reveal the overall status of trace metal contamination in various ecosystems, including soils (Jordanova et al., 2003; Spiteri et al., 2005; Yang et al., 2007a; Kapička et al., 2008; Blundell et al., 2009; Rosowiecka and Nawrocki, 2010), dusts (Kim et al., 2009; Yang et al., 2010; Bučko et al., 2010, 2011; Qiao et al., 2011; Wang et al., 2012; Zhang et al., 2012; Zhu et al., 2012), sediments/sludge (Chapparro et al., 2004; Yang et al., 2007b; Zhang et al., 2007, 2011; Rijal et al., 2010; Bijaksana and Huliselan, 2010), and plants (Matzka and Maher, 1999; Jordanova et al., 2003; Davila et al., 2006; Zhang et al., 2006; Maher et al., 2008; Salo et al., 2012). This use of magnetic techniques stems from the fact that heavy metal pollution in many cases is accompanied by emissions of ferromagnetic/ferrimagnetic particles because of the abundant presence of Fe in natural resource materials (Jordanova et al., 2003).

It is well known that stable Pb isotopes provide a useful means for identifying the origins of trace metals in the environment. This is because Pb derived from anthropogenic sources is less radiogenic than the geogenic Pb, and different sources of anthropogenic contaminants may contain Pb with characteristic isotopic compositions (Sangster et al., 2000).

Systematic assessment of trace metal contamination by the combined proxies (metal concentrations, magnetic parameters, and Pb isotopic ratios) has not been conducted before, which may provide detailed information about trace metal behaviors in urban environment. In the present study, atmospheric deposited dust samples were collected from kindergartens in a metropolis (Wuhan, China), and the concentrations of trace metals (i.e., Cd, Co, Cr, Cu, Ni, Pb, Zn, As, Sb, Ba, and Mo), magnetic parameters, and stable Pb isotopic compositions were fully investigated. The major objectives of this research are 1) to assess the contamination status and sources of trace metals in urban kindergarten dusts using magnetic, geochemical and lead isotopic analyses and 2) to explore the possible relationships between these different environmental proxies.

2. Materials and methods

2.1. Study area and sample collection

Wuhan (29°58'–31°22'N, 113°41'–115°05'E) is one of the biggest metropolises in China with an urban population of about 10.02 million in 2011. Its climate represents a typical subtropical humid monsoon with an average annual temperature of 17.7 °C and an average annual rainfall of 1300 mm. The prevailing wind is northeast wind in winter and south wind in summer. The number of kindergartens in this city is 638 with a total children population of 125,351 (WMBS, 2009).

Dust samples were collected from sixty-nine kindergartens in five districts, including Qingshan district (QS), Wuchang district (WC), Hankou district (HK), Hanyang district (HY), and Jiangxia district (JX) (Sun et al., 2013). QS is an industries concentrated area (including iron/steel smelters, machine manufacturing, and coal-power plants), WC is a commercial and education area, HK is a business and commercial area, HY is a residential area, and JX is a suburban district. Sampling was conducted in dry periods when no rain had occurred during the previous week. Approximately 50 g

dust sample was collected using polyethylene brush on impervious surface (children activities equipment, pavement and windowsill) from five to eight points of each kindergarten. All dust samples were stored in sealed polyethylene bags, labeled and then transported to the laboratory. The samples were air-dried at room temperature, and passed through a 1 mm sieve to remove rocks, plants, hair and other impurities. The homogenized dust samples were ground to a fine powder texture with an agate mortar prior to chemical analyses.

2.2. Experimental methods

Magnetic susceptibility (MS) at low (χ_{lf} , 976 Hz) and high (χ_{hf} , 15,616 Hz) frequencies were measured with a kappabridge MFK1-FA (AGICO, Brno) at 200 Am⁻¹ field intensity. Frequency-dependent susceptibility (χ_{fd}) was calculated and expressed as a percentage $\chi_{fd} \% = (\chi_{lf} - \chi_{hf})/\chi_{lf} \times 100\%$. An isothermal remanent magnetization (IRM) experiment was performed with an ASC Scientific (Model IM-10) impulse magnetizer and spinner magnetometer (Model SMD-88). The IRM acquired in a field of 1.0 T was regarded as saturation IRM (SIRM).

About 0.20 g of the prepared dust sample was digested with a concentrated HNO₃–HClO₄–HF–HCl mixture. The concentrations of trace metals of the digested solution were determined by an inductively coupled plasma–mass spectrometer (ICP–MS) (Finnigan MAT Element). For determination of As and Sb, the dust samples were digested with aqua regia (3:1, HCl:HNO₃) and determined by a hydride generation–atomic fluorescence spectrometer (HG–AFS) (AFS-920, Beijing Titan Instruments Co., Ltd.). QA/QC included reagent blanks, analytical duplicates, and analysis of the standard reference material (SRM) (SRM 2710). The recovery rates for the considered metals in the SRM were between 80 and 115%.

To determine the Pb isotopic composition, the solutions from the strong acid digestion were diluted to around 30 µg g⁻¹ Pb⁻¹ with 5% (v/v) high-purity HNO₃ and measured by ICP–MS (Perkin–Elmer Elan 6100 DRC^{plus}). The analytical parameters were sent as 190 sweeps/reading, one reading/replicate, and 10 replicates per sample solution. An international standard reference material (NIST SRM 981) was used for sample calibration and analytical control. The relative standard deviation (RSD) of the 10 replicates was generally below 0.5%. The measured ²⁰⁴Pb/²⁰⁷Pb, ²⁰⁶Pb/²⁰⁷Pb and ²⁰⁸Pb/²⁰⁷Pb ratios of SRM 981 were 0.0645 ± 0.0001, 1.0930 ± 0.0025 and 2.3702 ± 0.0050, which were in close agreement with the standard reference values of 0.0645, 1.0933, 2.3704, respectively.

2.3. Statistical analysis

The data were statistically analyzed using the statistical package, SPSS v13.0 (SPSS Inc.). A one-way ANOVA test ($p < 0.05$) was used to analyze the difference in analytical results among different urban areas. The correlation analysis was conducted by a Pearson correlation, and the level of significance was set at $p < 0.05$ and $p < 0.01$ (two-tailed). Principal component analysis (PCA) was conducted using factor extraction with eigenvalues >1 after varimax rotation.

Pollution status of the studied area was assessed using geoaccumulation index (I_{geo}) introduced by Muller (1969), which is calculated using the following equation:

$$I_{geo} = \log_2 \left[\frac{C_m \text{ Sample}}{(1.5 \times C_m \text{ Background})} \right]$$

Where $C_m \text{ Sample}$ is the measured concentration of the magnetic parameters or metals in dust, $C_m \text{ Background}$ is the geochemical

background value. In this study, the levels of the considered proxies of the soil dust samples collected from uncontaminated area were used as local geochemical background values, which are: χ $74 \times 10^{-8} \text{ m}^3 \text{ kg}^{-1}$, SIRM $12 \times 10^{-3} \text{ Am}^2 \text{ kg}^{-1}$, Pb 28 mg kg^{-1} , Zn 69 mg kg^{-1} , Cu 16 mg kg^{-1} , Cd 0.22 mg kg^{-1} , Cr 52 mg kg^{-1} , Ni 14 mg kg^{-1} , Co 6.0 mg kg^{-1} , As 12 mg kg^{-1} , Sb 1.1 mg kg^{-1} , Ba 321 mg kg^{-1} , and Mo 1.5 mg kg^{-1} . The factor 1.5 is introduced in this equation to minimize the effect of possible variations in the background values. According to Muller (1969), the I_{geo} is classified as: uncontaminated ($I_{\text{geo}} \leq 0$); uncontaminated to moderately contaminated ($0 < I_{\text{geo}} \leq 1$); moderately contaminated ($1 < I_{\text{geo}} \leq 2$); moderately to heavily contaminated ($2 < I_{\text{geo}} \leq 3$); heavily contaminated ($3 < I_{\text{geo}} \leq 4$); heavily to extremely contaminated ($4 < I_{\text{geo}} \leq 5$); extremely contaminated ($I_{\text{geo}} \geq 5$).

3. Results

3.1. Magnetic parameters

Magnetic parameters of the dust samples varied greatly among different urban areas (Table 1). The χ values of the whole sample set ranged from 83 to $2620 \times 10^{-8} \text{ m}^3 \text{ kg}^{-1}$. The enhancement of χ (mean $1510 \times 10^{-8} \text{ m}^3 \text{ kg}^{-1}$) in dust from industrial area (QS) was obvious compared to that from the other urban areas, whereas dust from suburban district (JX) had the lowest mean values of χ ($373 \times 10^{-8} \text{ m}^3 \text{ kg}^{-1}$). Similar to χ , the highest values of SIRM (mean $243 \times 10^{-3} \text{ Am}^2 \text{ kg}^{-1}$) were found in dust from QS, while the low values were obtained from HY (mean $57 \times 10^{-3} \text{ Am}^2 \text{ kg}^{-1}$) and JX (mean $50 \times 10^{-3} \text{ Am}^2 \text{ kg}^{-1}$). There was a significant correlation between SIRM and χ when the χ values were lower than $1000 \times 10^{-8} \text{ m}^3 \text{ kg}^{-1}$ ($r^2 = 0.891$, $p < 0.01$) (Fig. 1a), indicating that ferrimagnetic phases are the dominant magnetic minerals in these dust samples. However, such correlation was not observed for samples with high χ values ($>1000 \times 10^{-8} \text{ m}^3 \text{ kg}^{-1}$), which might be attributed to the presence of some ferromagnetic minerals (i.e., metallic iron) in these samples because the contributions of metallic iron to the intensity of SIRM and χ are different from the

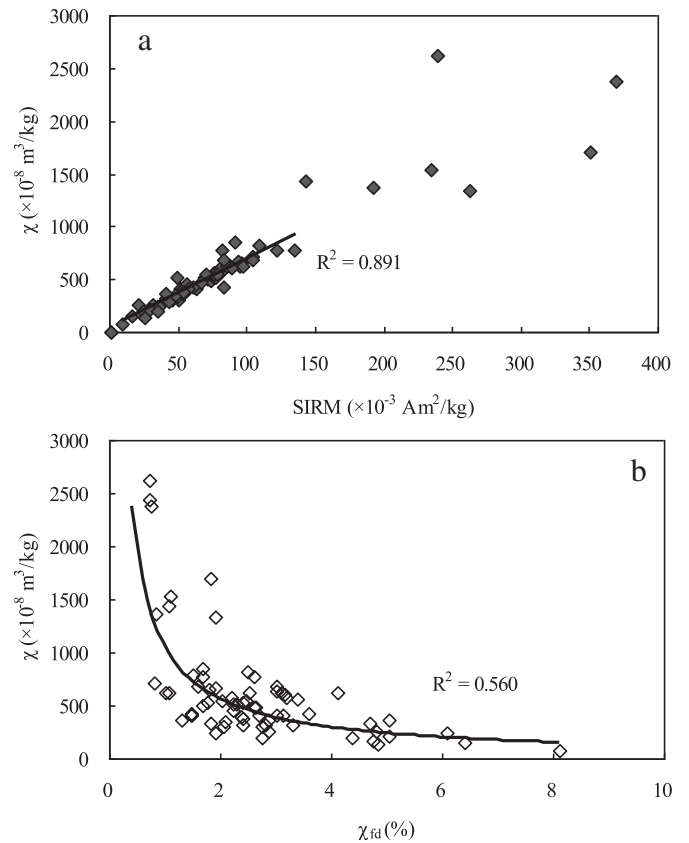


Fig. 1. Correlation scatter diagram between χ and SIRM (a) and between χ and χ_{fd} (b) in the dusts.

ferrimagnetic minerals (magnetite) (Zhang et al., 2010; Zhu et al., 2013).

The distribution of χ_{fd} among different urban areas was consistent with the results of χ and SIRM, which was increasing in

Table 1
Summary of magnetic properties and trace metal concentrations in the dusts.

		QS (n = 6)	WC (n = 27)	HK (n = 15)	HY (n = 8)	JX (n = 13)	Total (n = 69)
χ ($\times 10^{-8} \text{ m}^3 \text{ kg}^{-1}$)	Mean \pm SD	1510 \pm 560	594 \pm 432	623 \pm 548	437 \pm 181	373 \pm 338	621 \pm 511
	Median (range)	1490 (650–2380)	550 (136–2620)	493 (242–2440)	358 (256–849)	278 (83–1370)	497 (83–2620)
SIRM ($\times 10^{-3} \text{ Am}^2 \text{ kg}^{-1}$)	Mean \pm SD	243 \pm 109	81 \pm 41	77 \pm 47	57 \pm 18	50 \pm 49	86 \pm 70
	Median (range)	249 (96–370)	78 (26–240)	70 (35–224)	49 (32–91)	40 (9.5–193)	70 (9.5–370)
χ_{fd} (%)	Mean \pm SD	1.4 \pm 0.49	2.7 \pm 0.97	1.8 \pm 0.79	3.0 \pm 1.2	3.9 \pm 2.3	2.6 \pm 1.4
	Median (range)	1.5 (0.75–1.9)	2.6 (0.73–5.0)	1.9 (0.72–3.2)	2.8 (1.7–5.1)	3.6 (0.84–8.1)	2.4 (0.72–8.1)
Pb (mg kg ⁻¹)	Mean \pm SD	336 \pm 191	182 \pm 254	148 \pm 79	94 \pm 41	118 \pm 51	166 \pm 185
	Median (range)	369 (80–555)	126 (41–1440)	117 (49–310)	85 (41–164)	122 (45–200)	118 (41–1440)
Zn (mg kg ⁻¹)	Mean \pm SD	1250 \pm 889	450 \pm 173	633 \pm 471	321 \pm 131	321 \pm 147	518 \pm 427
	Median (range)	967 (363–2460)	442 (111–924)	480 (154–2060)	325 (130–541)	292 (122–623)	424 (111–2460)
Cu (mg kg ⁻¹)	Mean \pm SD	213 \pm 180	120 \pm 86	88 \pm 41	63 \pm 19	51 \pm 14	102 \pm 88
	Median (range)	137 (58–471)	99 (39–411)	78 (40–166)	70 (30–90)	48 (30–70)	70 (30–471)
Cd (mg kg ⁻¹)	Mean \pm SD	2.8 \pm 1.8	1.1 \pm 0.36	0.89 \pm 0.45	0.76 \pm 0.58	1.1 \pm 0.36	1.2 \pm 0.82
	Median (range)	3.4 (0.58–4.5)	1.1 (0.50–1.9)	0.86 (0.26–1.8)	0.57 (0.26–2.2)	1.0 (0.70–1.9)	1.0 (0.26–4.5)
Cr (mg kg ⁻¹)	Mean \pm SD	172 \pm 96	117 \pm 92	91 \pm 28	67 \pm 17	70 \pm 14	102 \pm 72
	Median (range)	150 (87–347)	90 (53–455)	83 (61–140)	61 (52–107)	68 (52–92)	82 (52–455)
Ni (mg kg ⁻¹)	Mean \pm SD	38 \pm 14	29 \pm 8.4	29 \pm 7.0	23 \pm 4.5	24 \pm 11	28 \pm 9.4
	Median (range)	35 (23–61)	28 (17–49)	28 (21–45)	23 (18–34)	21 (15–55)	26 (15–61)
Co (mg kg ⁻¹)	Mean \pm SD	20 \pm 12	11 \pm 2.5	10 \pm 1.7	9.4 \pm 1.6	11 \pm 1.9	11 \pm 4.6
	Median (range)	13 (11–39)	11 (7.4–18)	9.6 (7.8–15)	8.9 (7.5–12)	9.6 (8.3–15)	10 (7.4–39)
As (mg kg ⁻¹)	Mean \pm SD	32 \pm 20	15 \pm 4.2	14 \pm 4.1	12 \pm 1.3	16 \pm 2.3	16 \pm 8.2
	Median (range)	25 (16–72)	15 (9.5–29)	13 (9.8–24)	11 (10–14)	16 (13–21)	15 (9.5–72)
Sb (mg kg ⁻¹)	Mean \pm SD	7.9 \pm 5.6	4.6 \pm 2.1	4.8 \pm 1.7	3.9 \pm 2.0	3.0 \pm 1.3	4.5 \pm 2.5
	Median (range)	4.6 (3.3–16)	4.3 (1.4–10)	4.5 (2.3–7.9)	2.8 (1.8–7.5)	2.6 (2.0–6.5)	4.0 (1.4–16)
Ba (mg kg ⁻¹)	Mean \pm SD	1610 \pm 984	896 \pm 369	1050 \pm 360	708 \pm 138	823 \pm 311	951 \pm 469
	Median (range)	1350 (805–3430)	835 (402–2030)	873 (739–1900)	753 (531–895)	778 (383–1310)	844 (383–3430)
Mo (mg kg ⁻¹)	Mean \pm SD	7.2 \pm 3.9	3.9 \pm 1.9	2.9 \pm 1.1	3.1 \pm 2.3	2.7 \pm 0.64	3.6 \pm 2.1
	Median (range)	8.1 (2.8–11)	3.6 (1.8–11)	2.7 (1.4–5.2)	2.0 (1.1–8.2)	2.6 (1.9–3.9)	3.1 (1.1–11)

the following order: QS (1.4%) < HK (1.8%) < WC (2.7%) < HY (3.0%) < JX (3.9%). A clear trend of an increasing χ_{fd} with a decreasing χ was observed (Fig. 1b), which suggested that the coarse anthropogenic particles dominate the χ in the dust.

3.2. Trace metal concentrations

Eleven trace metals (Pb, Zn, Cu, Cd, Cr, Ni, Co, As, Sb, Ba, and Mo) were determined in this study (Table 1). For the whole studied areas, the concentrations of Pb and Zn had the widest ranges (more than 20 folds), from 41 to 1440 mg kg⁻¹ and from 111 to 2460 mg kg⁻¹, respectively, followed by Cd (0.26–4.5 mg kg⁻¹), Cu (30–471 mg kg⁻¹), Sb (1.4–16 mg kg⁻¹), and Mo (1.1–11 mg kg⁻¹), varying more than 10 folds. Whereas, relatively narrow ranges (<10 folds) of concentrations were found for Cr (52–455 mg kg⁻¹), Ni (15–61 mg kg⁻¹), Co (7.4–39 mg kg⁻¹), As (9.5–72 mg kg⁻¹), and Ba (383–3430 mg kg⁻¹). Among the five different urban areas, the highest concentrations of trace metals were consistently found in the industrial area (QS), while low metal concentrations were usually found in the residential area (HY) or suburban district (JX). Comparatively, dusts from commercial, business, and education comprehensive areas (HK and WC) had intermediate metal concentrations.

3.3. Pb isotopic compositions

Eleven samples with different Pb concentrations were selected for Pb isotope analysis. As shown in Table 2, the Pb isotopic ratios of the kindergarten dusts in Wuhan (except WC5) remained in a relatively narrow range, varying from 1.1548 to 1.1734 for ²⁰⁶Pb/²⁰⁷Pb and from 2.4582 to 2.4679 for ²⁰⁸Pb/²⁰⁷Pb, respectively. In the figure of ²⁰⁶Pb/²⁰⁷Pb vs ²⁰⁸Pb/²⁰⁷Pb (Fig. 2), all these data form a linear array ($R^2 = 0.498$, $p < 0.05$), suggesting the common origins of Pb in these dust samples. However, the sample of WC5 had an abnormal low Pb isotopic ratio (1.1125 for ²⁰⁶Pb/²⁰⁷Pb and 2.4457 for ²⁰⁸Pb/²⁰⁷Pb) as well as a high Pb concentration (1440 mg kg⁻¹), which differed greatly from the others.

4. Discussion

4.1. Contamination status

The significant correlation ($p < 0.01$) between magnetic parameters (χ and SIRM) and trace metal concentrations (Table 3) confirms that magnetic concentrations are sensitive to the enhancements of trace metals and thus can be used as a proxy to study metal contamination in urban environment. In the present

Table 2
Pb isotopic ratios of selected dust samples.

Sample no.	Pb concentration (mg kg ⁻¹)	Pb isotopic ratio		
		204/207	206/207	208/207
QS1	80	0.0632	1.1616	2.4676
QS2	396	0.0634	1.1627	2.4643
QS5	555	0.0637	1.1657	2.4637
QS6	140	0.0635	1.1635	2.4637
WC5	1440	0.0642	1.1125	2.4457
WC12	329	0.0641	1.1583	2.4592
HK4	310	0.0636	1.1562	2.4582
HK6	226	0.0634	1.158	2.4647
HY6	41	0.0641	1.1734	2.4664
JX6	134	0.0639	1.1548	2.4605
JX10	83	0.0636	1.1682	2.4679

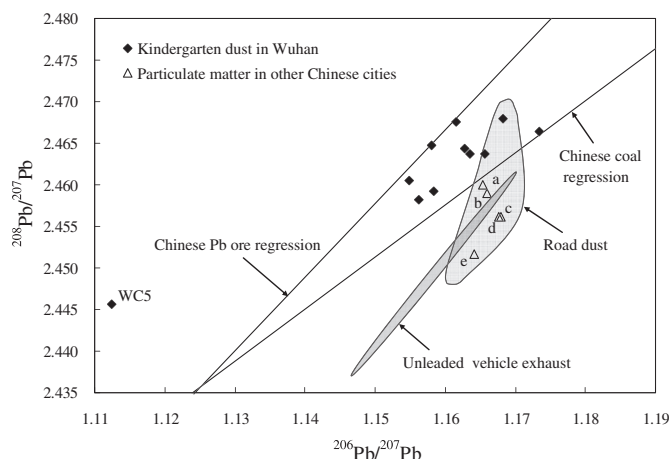


Fig. 2. ²⁰⁶Pb/²⁰⁷Pb vs ²⁰⁸Pb/²⁰⁷Pb in kindergarten dusts in comparison with literature data. The Chinese Pb ore line and coal line were obtained from the linear regression of data from Zhu et al. (2001), Gao et al. (2004), Zheng et al. (2004), Tan et al. (2006) and Cheng and Hu (2010). The data of road dust collected in Guangzhou are from Duzgoren-Aydin (2007), the data of unleaded vehicle exhausts are from Gao et al. (2004) and Tan et al. (2006). Lower case letters indicate data in airborne particles from Chinese cities: a, Hefei (Ewing et al., 2010); b, Xiameng (Zhu et al., 2010); c, Guiyang (Li et al., 2012); d, Guangzhou (Lee et al., 2007); e, Shanghai (Tan et al., 2006).

study, both magnetic properties and trace metal concentrations can reveal the intensities of various anthropogenic activities in different urban areas (Table 1). The contamination status of trace metals can be clearly reflected by the geoaccumulation index (I_{geo}) (Fig. 3). As shown in Fig. 3, the contamination extent of trace metals in different urban areas was in the following order: QS > HK = WC > HY ≥ JX. Zn, Pb, Cu, Cd, and Sb were the major metal pollutants in the city, characterized by moderately to heavily contaminate ($I_{geo} = 1-4$). Comparatively, the contamination of Ba, Mo, Co, Cr, Ni, and As was less heavy (uncontaminated to moderately contaminated) ($I_{geo} < 1$). In comparison with individual metals, the I_{geo} values of magnetic properties were more prominent (Fig. 3). This is due to the fact that magnetic properties can reveal the integrated loading of the whole metal pollutants instead of individual metals (Kim et al., 2007). Therefore the contamination situation of different urban areas can be more easily summarized and classified by magnetic concentrations than by individual metals.

Magnetic parameter (χ) and the most common metal pollutants (Zn, Pb, and Cu) in the dust of this study were compared with those in other cities around the world (Fig. 4). The levels of χ and trace metals in the present study were higher than that of the street dusts from the common Chinese cities of Xi'an (Li et al., 2010), Beijing (Qiao et al., 2011), Lanzhou (Wang et al., 2012), and Chibi (Liu et al., 2009), and park road dust from Wuhan (Yang et al., 2011), but lower than that of the street dusts from the industrial cities of Baoji (Wang, 2008) and Loudi (Zhang et al., 2012). In comparison with data from Hong Kong (Ng et al., 2003; Chan et al., 2006) and Seoul (Kim et al., 2007), the value of χ in this study was higher, but the trace metal concentrations were lower. It is interesting to note that the data sets from the cities in mainland China form a linear relationship ($R^2 = 0.875$, $p < 0.01$) and differ from those of Hong Kong and Seoul. This suggested that magnetic particles and trace metals in Chinese urban settings widely coexisted and were derived from the sources with similar MS to metal ratios. It is therefore possible to use the ratios of MS/metal as an indicator for identification of pollution sources between Chinese cities and the other Asian cities.

Table 3Pearson's correlation coefficients (r) between magnetic properties (χ , SIRM, and χ_{fd}) and trace metals.

	Pb	Zn	Cu	Cd	Cr	Ni	Co	As	Sb	Ba	Mo
χ	0.603**	0.558**	0.583**	0.403**	0.650**	0.568**	0.568**	0.542**	0.391**	0.381**	0.680**
SIRM	0.765**	0.564**	0.641**	0.578**	0.611**	0.601**	0.737**	0.686**	0.586**	0.396**	0.776**
χ_{fd}	-0.360**	-0.338**	-0.290*	-0.180	-0.292*	-0.351**	-0.148	-0.133	-0.247*	-0.319**	-0.287*

*Significant level at $p < 0.05$ (two-tailed).**Significant level at $p < 0.01$ (two-tailed).

4.2. Sources identification

4.2.1. By Pb isotopic ratios

It is evident that anthropogenic Pb in urban environments is commonly derived from traffic related emissions, combustion of coal, and resource (mainly Pb–Zn ores) consumption in various industries including metallurgy, hardware, plastic, ceramic, and mining. In comparison with Pb isotopes of aerosol in other Chinese cities, the Pb isotopic compositions of urban kindergarten dusts in Wuhan were characterized by higher ^{208}Pb component (Fig. 2). As shown in Fig. 2, all data points (except sample WC5) of this study were plotted between the regression lines of Chinese Pb ores and

coals, suggesting that Pb in the dusts was mainly derived from industrial emissions and coal combustion. On the contrary, our data set shifted away from the Pb isotopic signatures of unleaded vehicle exhaust and road dust (representing combined vehicle exhaust and non-exhaust sources), indicating that the contribution of traffic related emissions was not significant. This result is in agreement with those from many previous studies which reported that traffic emissions were no longer a predominant source of Pb in urban environment after the phasing out of leaded gasoline (e.g., Zheng et al., 2004; Tan et al., 2006; Zhu et al., 2010). Furthermore, some researches demonstrated that vehicular derived metal pollutants were unlikely to disperse far away from the emission sources (Hoffmann et al., 1999; Blundell et al., 2009; Bi et al., 2013). Our on-site investigation showed that there was a certain distance (generally >50 m) between most of the sampled kindergartens and the main roads. Therefore, the influences of traffic emissions on Pb concentrations in the dust might be insignificant.

Besides the above recognized Pb sources, there were also unknown pollution sources in the studied city. For example, the sample WC5 had a distinctly low radiogenic Pb composition and plotted far away from the others. Meanwhile, this sample had a high concentration of Pb. This might indicate that this site had previously been used in another capacity.

The relationship between the Pb concentrations and $^{206}\text{Pb}/^{207}\text{Pb}$ ratios is shown in Fig. 5 (excluding the data of WC5). There would be a negative correlation between the level of Pb contamination and the $^{206}\text{Pb}/^{207}\text{Pb}$ ratios if the direct contributions of Pb were from the source(s) having distinctively less radiogenic isotopic signatures. As shown in Fig. 5, the negative correlation was found when the Pb concentrations were at a relatively low level (e.g., <300 mg kg^{-1}), however this correlation was reversed when the Pb concentrations were higher than 300 mg kg^{-1} . This again indicated that there were at least two sources of Pb in the urban dusts from Wuhan. One had relatively low $^{206}\text{Pb}/^{207}\text{Pb}$ ratios (~ 1.155) and moderate Pb concentrations, which might represent the coal combustion source considering the moderate Pb concentrations in coal fly ash (Ren et al., 2006). The other had slightly elevated $^{206}\text{Pb}/^{207}\text{Pb}$ ratios (~ 1.165) and high Pb concentrations, which

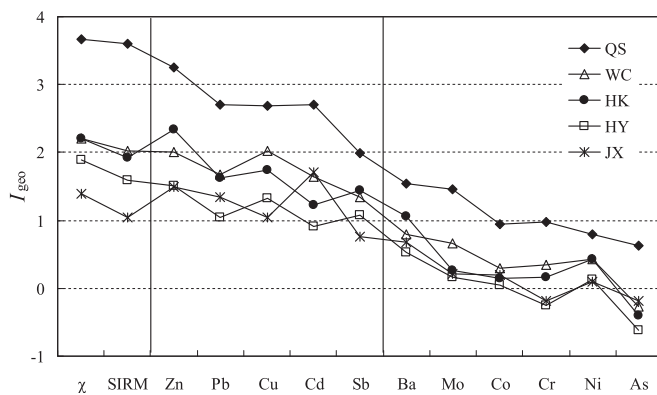


Fig. 3. Geoaccumulation index (I_{geo}) of χ , SIRM, and trace metals in the dusts from different urban areas.

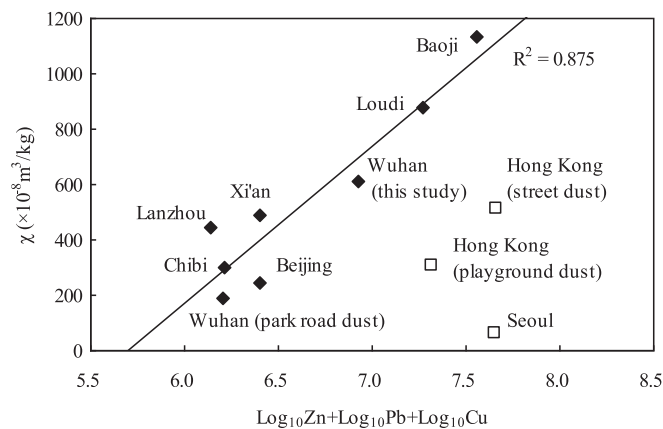


Fig. 4. Correlation scatter diagram between χ and the sum of Zn, Pb, and Cu concentrations (mean values from each studied area). The metal concentrations were Log normalized to eliminate the big variation between metals. The data sets were obtained in kindergarten dusts from Wuhan (this study), street dusts from Baoji (Wang, 2008), Loudi (Zhang et al., 2012), Xi'an (Li et al., 2010), Beijing (Qiao et al., 2011), Lanzhou (Wang et al., 2012), Chibi (Liu et al., 2009), Hong Kong (Chan et al., 2006), and Seoul (Kim et al., 2007), park road dust from Wuhan (Yang et al., 2011), and playground dust from Hong Kong (Ng et al., 2003).

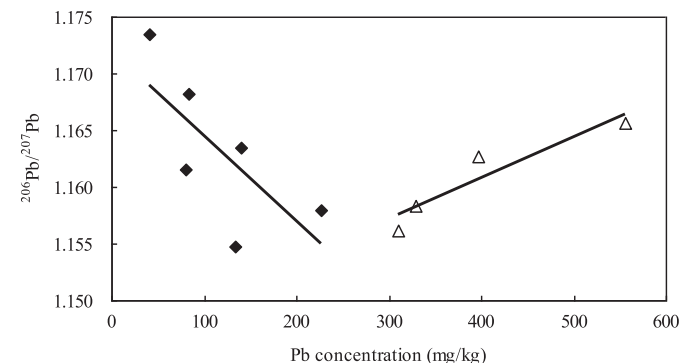


Fig. 5. The distribution of Pb concentrations and $^{206}\text{Pb}/^{207}\text{Pb}$ ratios in the dusts.

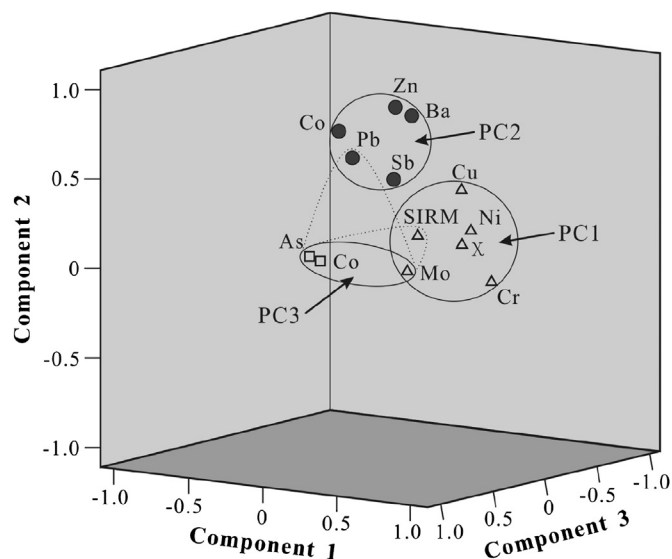


Fig. 6. PCA results of the kindergarten dust samples in the three-dimensional space.

might represent the industrial sources because industrial activities always release high levels of metal pollutants (Bi et al., 2013; Zhang et al., 2011, 2012). Indeed, the dust samples (QS2 and QS 5) having high Pb concentrations (396 and 555 mg kg^{-1} , respectively) were just from the industrial area (Table 2 and Fig. 5).

4.2.2. By PCA analysis

Principal component analysis (PCA) is a useful method to identify anthropogenic pollution sources in different urban settings. The metal composition, together with the magnetic properties (χ and SIRM), was dominated by three principal components (PCs) that explained 74.4% of the total variances (Fig. 6). PC1 explained 50.8% of the total variances with high loadings of Cu, Cr, Ni, Mo, χ , and SIRM. PC2 was associated with Pb, Zn, Cd, Ba, and Sb, accounting for 13.6% of the variances. PC3 showed high factor loadings on As, Co, and Mo, accounting for 10.2% of the variances. Pb (0.605) and SIRM (0.564) also showed relatively higher values in PC3.

Cr, Ni, Cu, and Mo in PC1 may indicate the influence of iron/steel smelting and processing activities since they are the principal industries in the studied city. The highest affinity of magnetic properties (χ and SIRM) with this component confirmed the contribution of the iron/steel related industries (Zhang et al., 2011, 2012). The association of the trace metals of Pb, Zn, Cd, Ba, and Sb in PC2 is likely related to the influence of traffic emission sources and/or non-ferrous metal production (Nriagu and Pacyna, 1988; Pacyna and Pacyna, 2001; Adachi and Tainosho, 2004; Duzgoren-Aydin et al., 2006; Duong and Lee, 2011). However, the aforementioned Pb isotopic ratios have already ruled out the contribution of traffic sources. So, the PC2 can only represent the sources of non-ferrous metal related industries. The PC3, represented by As, Co, and Mo, may be an indicator of the coal combustion source since the coal burning emission is regarded as an important source of As and Mo in urban environment (Nriagu and Pacyna, 1988; Pacyna and Pacyna, 2001; Ren et al., 2006; Lu et al., 2009). Pb was also associated with PC3, which was in agreement with the Pb isotopic results and confirmed that coal combustion was an important source of Pb in the studied city. The relatively higher correlation of SIRM with PC3 was reasonable because coal fly ashes usually contained a substantial amount of magnetic spherules (Magiera et al., 2011).

Overall, PCA suggested that multiple anthropogenic sources regulated the elemental compositions of the urban environment (Duzgoren-Aydin et al., 2006). According to the results of PCA, the

metal pollutants in the kindergarten dusts from Wuhan can be classified into three major groups/sources: (1) Cr, Ni, Cu, and Mo – iron/steel smelting and processing industries; (2) Pb, Zn, Cd, Ba, and Sb – non-ferrous metal related industries; (3) As, Co, Mo, and Pb – coal combustion. Since the MS and SIRM are sensitive to some specific anthropogenic activities (iron/steel smelting and coal combustion), the incorporation of magnetic properties into PCA could prove to be more persuasive in the identification of pollution sources.

5. Conclusion

Magnetic properties and trace metal concentrations in the kindergarten dusts from Wuhan varied greatly between different urban areas with the highest values in industrial area and low values in residential area or suburban district. The significant correlation between magnetic parameters and trace metal concentrations indicated that the magnetic method is a useful tool for identification of metal pollution. Our results also revealed that the contamination status of different urban areas can be more easily summarized and classified by magnetic concentrations than by individual metals. Furthermore, the magnetic susceptibility (MS) and trace metals (Zn, Pb, and Cu) in our study together with published results from other Chinese cities formed a linear relationship, suggesting that magnetic particles and trace metals in Chinese urban areas widely coexisted and were derived from the sources with similar MS to metal ratios. The results of stable Pb isotopic ratios (1.1548 – 1.1734 for $^{206}\text{Pb}/^{207}\text{Pb}$ and 2.4582 – 2.4679 for $^{208}\text{Pb}/^{207}\text{Pb}$) and PCA indicated that metal pollutants in the kindergarten dusts from Wuhan can be classified into three major groups/sources: (1) Cr, Ni, Cu, and Mo – iron/steel smelting and processing industries; (2) Pb, Zn, Cd, Ba, and Sb – non-ferrous metal related industries; (3) As, Co, Mo, and Pb – coal combustion. The results of the present study demonstrated that in comparison with the single technique, the combined application of multi-proxies could provide more detailed and accurate information on metal distribution and origination in urban environment.

Acknowledgments

This study was financial supported by the Natural Science Foundation of China (40904015 and 41273003).

References

- Adachi, K., Tainosho, Y., 2004. Characterization of heavy metal particles embedded in tire dust. *Environment International* 30, 1009–1017.
- Bi, X.Y., Liang, S.Y., Li, X.D., 2013. Trace metals in soil, dust, and tree leaves of the urban environment, Guangzhou. *Chinese Science Bulletin* 58, 222–230.
- Bijaksana, S., Huliselan, E.K., 2010. Magnetic properties and heavy metal content of sanitary leachate sludge in two landfill sites near Bandung, Indonesia. *Environmental Earth Science* 60, 409–419.
- Blundell, A., Hannam, J.A., Dearing, J.A., Boyle, J.F., 2009. Detecting atmospheric pollution in surface soils using magnetic measurements: a reappraisal using an England and Wales database. *Environmental Pollution* 157, 2878–2890.
- Bučko, M.S., Magiera, T., Pesonen, L.J., Janus, B., 2010. Magnetic, geochemical, and microstructural characteristics of road dust on roadsides with different traffic volumes – case study from Finland. *Water, Air, and Soil Pollution* 209, 295–306.
- Bučko, M.S., Magiera, T., Johanson, B., Petrovský, E., Pesonen, L.J., 2011. Identification of magnetic particulates in road dust accumulated on roadside snow using magnetic, geochemical and micro-morphological analyses. *Environmental Pollution* 159, 1266–1276.
- Chan, M.K., Chan, L.S., Ng, S.L., Liu, Q.S., 2006. Heavy metal contents and magnetic properties of street dust in two districts of different traffic density in Hong Kong. *Geophysical Solutions for Environment and Engineering* 1–2, 807–811.
- Chapparro, M.A.E., Bidegain, J.C., Sinito, A.M., Jurado, S.S., Gogorza, C.S.G., 2004. Relevant magnetic parameters and heavy metals from relatively polluted stream sediments – vertical and longitudinal distribution along a cross-city stream in Buenos Aires Province, Argentina. *Studia Geophysica Geodaetica* 48, 615–636.

- Chen, J.M., Tong, Y.P., Xu, J.Z., Liu, X.L., Li, Y.L., Tan, M.G., Li, Y., 2012. Environmental lead pollution threatens the children living in the Pearl River Delta region, China. *Environmental Science Pollution Research* 19, 3268–3275.
- Cheng, H., Hu, Y., 2010. Lead (Pb) isotopic fingerprinting and its applications in lead pollution studies in China: a review. *Environment Pollution* 158, 1134–1146.
- Davila, A.F., Rey, D., Mohamed, K., Rubio, B., Guerra, A.P., 2006. Mapping the sources of urban dust in a coastal environment by measuring magnetic parameters of *Platanus hispanica* leaves. *Environmental Science and Technology* 40, 3922–3928.
- Duong, T.T.T., Lee, B.K., 2011. Determining contamination level of heavy metals in road dust from busy traffic areas with different characteristic. *Journal of Environmental Management* 92, 554–562.
- Duzgoren-Aydin, N.S., 2007. Sources and characteristics of lead pollution in the urban environment of Gusngzhou. *Science of the Total Environment* 385, 182–195.
- Duzgoren-Aydin, N., Wong, C.S.C., Aydin, A., Song, Z., You, M., Li, X.D., 2006. Heavy metal contamination and distribution in the urban environment of Guangzhou, SE China. *Environmental Geochemistry and Health* 28, 375–391.
- Ewing, S.A., Christensen, J.N., Brown, S.T., Vancuren, R.A., Cliff, S.S., Depaolo, D.J., 2010. Pb isotopes as an indicator of the Asian contribution to particulate air pollution in urban California. *Environmental Science and Technology* 44, 8911–8916.
- Ferreira-Baptista, L., De Miguel, E., 2005. Geochemistry and risk assessment of street dust in Luanda, Angola: a tropical urban environment. *Atmospheric Environment* 39, 4501–4512.
- Gao, Z.Y., Yin, G., Ni, S.J., Zhang, C.J., 2004. Geochemical feature of the urban environmental lead isotope in Chendu city. *Carologica Sinica* 4, 267–272.
- Hoffmann, V., Knab, M., Appel, E., 1999. Magnetic susceptibility mapping of roadside pollution. *Journal of Geochemical Exploration* 66, 313–326.
- Jordanova, N.V., Jordanova, D.V., Veneva, L., Yorova, K., Petrovsky, E., 2003. Magnetic response of soils and vegetation to heavy metal pollution – a case study. *Environmental Science and Technology* 37, 4417–4424.
- Kapicka, A., Petrovský, E., Fialová, H., Podrázský, V., Dvořák, I., 2008. High resolution mapping of anthropogenic pollution in the Giant Mountains National Park using soil magnetometry. *Studia Geophysica Geodaetica* 52, 271–284.
- Kim, W., Doh, S.J., Park, Y.H., Yun, S.T., 2007. Two-year magnetic monitoring in conjunction with geochemical and electron microscopic data of roadside dust in Seoul, Korea. *Atmospheric Environment* 41, 7627–7641.
- Kim, W., Doh, S.J., Yu, Y., 2009. Anthropogenic contribution of magnetic particulates in urban roadside dust. *Atmospheric Environment* 43, 3137–3144.
- Laidlaw, M.A.S., Taylor, M.P., 2011. Potential for childhood lead poisoning in the inner cities of Australia due to exposure to lead in soil dust. *Environmental Pollution* 159, 1–9.
- Laidlaw, M.A.S., Mielke, H.W., Filippelli, G.M., Johnson, D.L., Gonzales, C.R., 2005. Seasonality and children's blood lead levels: developing a predictive model using climatic variables and blood lead data from Indianapolis, Indiana, Syracuse, New York, and New Orleans, Louisiana (USA). *Environmental Health Perspectives* 113 (6), 793–800.
- Lee, C.S.L., Li, X.D., Zhang, G., Li, J., Ding, A.J., Wang, T., 2007. Heavy metals and Pb isotopic composition of aerosols in urban and suburban areas of Hong Kong and Guangzhou, South China – evidence of the long-range transport of air contaminants. *Atmospheric Environment* 41, 432–447.
- Li, P., Qiang, X., Tang, Y., Fu, C., Xu, X., Li, X., 2010. Magnetic susceptibility of the dust of street in Xi'an and the implication on pollution. *China Environment Science* 30, 309–314 (in Chinese).
- Li, F.L., Liu, C.Q., Yang, Y.G., Bi, X.Y., Liu, T.Z., Zhao, Z.Q., 2012. Natural and anthropogenic lead in soils and vegetables around Guiyang city, southwest China: a Pb isotopic approach. *Science of the Total Environment* 431, 339–347.
- Liu, Q.S., Zeng, Q.L., Yao, T., Qiu, N., Chan, L.S., 2009. Magnetic properties of street dust from Chibi city, Hubei province, China: its implications for urban environment. *Journal of Earth Science* 20, 848–857.
- Lu, X.W., Li, L.Y., Wang, L.J., Lei, K., Huang, J., Zhai, Y.X., 2009. Contamination assessment of mercury and arsenic in roadway dust from Baoji, China. *Atmospheric Environment* 43, 2489–2496.
- Magiera, T., Jabłońska, M., Strzyszczyk, Z., Rachwał, M., 2011. Morphological and mineralogical forms of technogenic magnetic particles in industrial dusts. *Atmospheric Environment* 45, 4281–4290.
- Maher, B.A., Moore, C., Matzka, J., 2008. Spatial variation in vehicle-derived metal pollution identified by magnetic and elemental analysis of roadside tree leaves. *Atmospheric Environment* 42, 364–373.
- Matzka, J., Maher, B.A., 1999. Magnetic biomonitoring of roadside tree leaves: identification of spatial and temporal variations in vehicle-derived particulates. *Atmospheric Environment* 33, 4565–4569.
- Muller, G., 1969. Index of geoaccumulation in sediments of the Rhine River. *Geological* 2, 108–118.
- Ng, S.L., Chan, L.S., Lam, K.C., Chan, W.K., 2003. Heavy metal contents and magnetic properties of playground dust in Hong Kong. *Environmental Monitoring and Assessment* 89, 221–232.
- Nriagu, J.O., Pacyna, J.M., 1988. Quantitative assessment of worldwide contamination of air, water and soils by trace metals. *Nature* 333, 134–139.
- Pacyna, J.M., Pacyna, E.G., 2001. An assessment of global and regional emissions of trace metals to the atmosphere from anthropogenic sources worldwide. *Environmental Reviews* 9, 269–298.
- Qiao, Q., Zhang, C., Huang, B., Piper, J.D.A., 2011. Evaluating the environmental quality impacted of the 2008 Beijing Olympic games: magnetic monitoring of street dust in Beijing Olympic Park. *Geophysical Journal International* 187, 1222–1236.
- Ren, D.Y., Zhao, F.H., Dai, S.F., Zhang, J.Y., Luo, K.L., 2006. *Geochemistry of Trace Elements in Coal*. Science Press, Beijing, China.
- Rijal, M.L., Appel, E., Petrovský, E., Blaha, U., 2010. Change of magnetic properties due to fluctuations of hydrocarbon contaminated groundwater in unconsolidated sediments. *Environmental Pollution* 158, 1756–1762.
- Roels, H.A., Buchet, J.-P., Lauwerys, R.R., Bruaux, P., Claeys-Thoreau, F., Lafontaine, A., Verduyn, G., 1980. Exposure to lead by the oral and the pulmonary routes of children living in the vicinity of a primary lead smelter. *Environmental Research* 22, 81–94.
- Rosowiecka, O., Nawrocki, J., 2010. Assessment of soils pollution extent in surroundings of ironworks based on magnetic analysis. *Studia Geophysica Geodaetica* 54, 185–194.
- Salo, H., Bučko, M.S., Vaahtovuori, E., Limo, J., Mäkinen, J., Pesonen, L.J., 2012. Bio-monitoring of air pollution in SW Finland by magnetic and chemical measurements of moss bags and lichens. *Journal of Geochemical Exploration* 115, 69–81.
- Sangster, D.F., Ouditridge, P.M., Davis, W.J., 2000. Stable lead isotope characteristics of lead ore deposits of environmental significance. *Environmental Research* 8, 115–147.
- Soto-Jiménez, M.F., Flegal, A.R., 2011. Childhood lead poisoning from the smelter in Torreón, México. *Environmental Research* 111, 590–596.
- Spiteri, C., Kalinski, V., Rösler, W., Hoffmann, V., Appel, E., 2005. Magnetic screening of a pollution hotspot in the Lausitz area, Eastern Germany: correlation analysis between magnetic proxies and heavy metal contamination in soils. *Environmental Geology* 49, 1–9.
- Sun, G., Li, Z., Bi, X., Chen, Y., Lu, S., Yuan, X., 2013. Distribution, sources and health risk assessment of mercury in kindergarten dust. *Atmospheric Environment* 73, 169–176.
- Tan, M.G., Zhang, G.L., Li, X.L., Zhang, Y.X., Yue, W.S., Chen, J.M., Wang, Y.S., Li, A.G., Li, Y., Zhang, Y.M., Shan, Z.C., 2006. Comprehensive study of lead pollution in Shanghai by multiple techniques. *Analytic Chemistry* 78, 8044–8050.
- Wang, L.J., 2008. *Heavy Metal Contamination in Street Dusts, Soil, and Weihe Sediments From Baoji*. Master's thesis. Shaanxi Normal University.
- Wang, G., Oldfield, F., Xia, D., Chen, F., Liu, X., Zhang, W., 2012. Magnetic properties and correlation with heavy metals in urban street dust: a case study from the city of Lanzhou, China. *Atmospheric Environment* 46, 289–298.
- WMBS (Wuhan Municipal Bureau of Statistics), 2009. *Statistical Yearbook of Wuhan City*. China Statistics Press, Beijing.
- Yang, T., Liu, Q., Chan, L., Cao, G., 2007a. Magnetic investigation of heavy metals contamination in urban topsoils around the East Lake, Wuhan, China. *Geophysical Journal International* 171, 603–612.
- Yang, T., Liu, Q., Chan, L., Chan, L., Liu, Z., 2007b. Magnetic signature of heavy metals pollution of sediments: case study from the East Lake in Wuhan, China. *Environmental Geology* 52, 1639–1650.
- Yang, T., Liu, Q., Li, H., Zeng, Q., Chan, L., 2010. Anthropogenic magnetic particles and heavy metals in the road dust: magnetic identification and its implications. *Atmospheric Environment* 44, 1175–1185.
- Yang, T., Zeng, Q., Liu, Z., Liu, Q., 2011. Magnetic properties of the road dusts from two parks in Wuhan city, China: implications for mapping urban environment. *Environmental Monitoring and Assessment* 177, 637–648.
- Zhang, C., Huang, B., Li, Z., Liu, H., 2006. Magnetic properties of highroad-side pine tree leaves in Beijing and their environmental significance. *Chinese Science Bulletin* 51, 3041–3052.
- Zhang, W., Yu, L., Lu, M., Hutchinson, S.M., Feng, H., 2007. Magnetic approach to normalizing heavy metal concentrations for particle size effects in intertidal sediments in the Yangtze Estuary, China. *Environmental Pollution* 147, 238–244.
- Zhang, C., Liu, Q., Huang, B., Su, Y., 2010. Magnetic enhancement upon heating of environmentally polluted samples containing haematite and iron. *Geophysical Journal International* 181, 1381–1394.
- Zhang, C., Qiao, Q., Piper, J.D.A., Huang, B., 2011. Assessment of heavy metal pollution from a Fe-smelting plant in urban river sediments using environmental magnetic and geochemical methods. *Environmental Pollution* 159, 3057–3070.
- Zhang, C., Qiao, Q., Appel, E., Huang, B., 2012. Discriminating sources of anthropogenic heavy metals in urban street dusts using magnetic and chemical methods. *Journal of Geochemical Exploration* 119–120, 60–75.
- Zheng, J., Tan, M., Shibata, Y., Tanaka, A., Li, Y., Zhang, G., Zhang, Y., Shan, Z., 2004. Characteristics of lead isotope ratios and elemental concentrations in PM₁₀ fraction of airborne particulate matter in Shanghai after the phase-out of leaded gasoline. *Atmospheric Environment* 38, 1191–1200.
- Zheng, N., Liu, J., Wang, Q., Liang, Z., 2010. Health risk assessment of heavy metal exposure to street dust in the zinc smelting district, Northeast of China. *Science of the Total Environment* 408, 726–733.
- Zhu, B.Q., Chen, Y.W., Peng, J.H., 2001. Lead isotope geochemistry of the urban environment in the Pearl River Delta. *Applied Geochemistry* 16, 409–417.
- Zhu, L.M., Tang, J.W., Lee, B., Zhang, Y., Zhang, F.F., 2010. Lead concentrations and isotopes in aerosols from Xiamen, China. *Marine Pollution Bulletin* 60, 1946–1955.
- Zhu, Z., Han, Z., Bi, X., Yang, W., 2012. The relationship between magnetic parameters and heavy metal contents of indoor dust in e-waste recycling impacted area, Southeast China. *Science of the Total Environment* 433, 302–308.
- Zhu, Z., Li, Z., Bi, X., Han, Z., Yu, G., 2013. Response of magnetic properties to heavy metal pollution in dust from three industrial cities in China. *Journal of Hazardous Materials* 246–247, 189–198.